Quantum Electronics **39** (10) 962 – 966 (2009)

LASER APPLICATIONS AND OTHER TOPICS IN QUANTUM ELECTRONICS

PACS numbers: 42.62.Cf; 42.25.Fx; 47.80.Cb; 47.80.Jk
DOI: 10.1070/QE2009v039n10ABEH014054

Laser Doppler visualisation of the velocity field by excluding the influence of multiparticle scattering

Yu.N. Dubnishchev, Yu.V. Chugui, J. Kompenhans

***Abstract*. The method of laser Doppler visualisation and measurement of the velocity field in gas and liquid flows by suppressing the influence of multiparticle scattering is discussed. The cross section of the flow under study is illuminated by a laser beam transformed by an anamorphic optical system into a laser sheet. The effect of multiparticle scattering is eliminated by obtaining differential combinations of frequency-demodulated images of the laser sheet in different regions of the angular spectrum of scattered light.**

Keywords: *laser Doppler visualisation of the velocity field, multiparticle scattering of light, optical mixing spectroscopy, Doppler global velocimetry.*

1. Introduction

One of the major fields of laser applications is optical diagnostics of gas and liquid flows [1 – 3]. Laser Doppler visualisation and measurement of the velocity field were proposed in [4]. This method is based on illumination of the flow cross section by a laser beam transformed by an anamorphic optical system into a laser sheet, whose image in the frequency-demodulated scattered light maps the distribution of the Doppler frequency shift in this cross section and, hence, projections of the velocity vector on the direction specified by the difference of the wave vectors $\boldsymbol{k}_{\rm s} - \boldsymbol{k}$, where $\boldsymbol{k}$ and $\boldsymbol{k}_{\rm s}$ are the wave vectors of the laser sheet and scattered light beam. As an optical frequency demodulator performing the frequency – intensity conversion, a gas cell is employed, in which the absorption band slope is used as a discrimination curve. The possibility of using optical dispersion media as frequency – intensity converters was also considered. In papers [5 – 9], the frequency demodulator was a coherent-feedback Doppler processor based on a semiconfocal resonator matched with the mode structure of laser radiation producing the laser sheet. The influence of the scattered light intensity fluctuations was eliminated in paper [10] by normalising the signal image to the reference one, which was not subjected to frequency demodulation. A separate CCD camera was used to detect the reference image in this paper, while the frequency – intensity converter was an absorbing iodine-vapour cell. The method of laser Doppler measurement of the velocity field by using one CCD camera, a molecular absorption cell, and the frequency modulation of the laser sheet is described in [11]. It was shown that the velocity field could be measured from the amplitude ratio of the first and second harmonics of the modulation frequency. These harmonics appear upon the frequency discrimination of the scattered light field by the frequency – intensity converter with the nonlinear transfer function.

The general disadvantage of the described methods of laser Doppler visualisation and measurement of the velocity field, historically termed Doppler global velocimetry (DGV), is the influence of multiparticle scattering in the laser sheet on the measurement results, especially at high concentrations of scattering particles. In this paper, we discuss the possibility of minimising this influence.

2. Laser Doppler visualisation and measurement of the velocity fields by excluding the influence of multiparticle scattering

Consider the concept of the laser Doppler measurement of the velocity field by excluding the influence of multiparticle scattering for DGV systems with a reference CCD camera and systems in which the velocity field is recorded with one camera.

2.1 Laser Doppler visualisation of the velocity fields by using a reference CCD camera

The vector scheme in Fig. 1 illustrates the proposed method for eliminating the influence of multiparticle scattering on the results of measurement of the velocity field. The laser sheet is formed by an incident light field with the wave vector $\boldsymbol{k}$. Consider the light field $\tilde{E}_{n1}$ scattered by the nth particle in the direction of the wave vector $\boldsymbol{k}_{\rm s1}$, taking into account the light, scattered from the adjacent mth particle, which is incident on this nth particle. This light field can be represented in the form

$$\tilde{E}_{n1} = AS_{n1}\exp\{{\rm i}\{[\omega_0 + \Omega + \boldsymbol{v}_n(\boldsymbol{k}_{\rm s1} - \boldsymbol{k})]t + \varphi_n\}\} +$$

$$+ A\sum_m S_{nm1}\exp\{{\rm i}\{[\omega_0 + \Omega + \boldsymbol{v}_m(\boldsymbol{k}_{nm} - \boldsymbol{k})-$$

Yu.N. Dubnishchev Institute of Thermophysics, Siberian Branch, Russian Academy of Sciences, prosp. Akad. Lavrent'eva 1, 630090 Novosibirsk, Russia; e-mail: dubnistchev@itp.nsc.ru;
Yu.V. Chugui Technological Design Institute of Scientific Instrument Engineering, Siberian Branch, Russian Academy of Sciences, ul. Russkaya 41, 630058 Novosibirsk, Russia;
J. Kompenhans German Aerospace Center, Bunsenstrasse 10, 37073 Göttingen, Germany

Received 26 January 2009; revision received 5 May 2009
Kvantovaya Elektronika **39** (10) 962 – 966 (2009)
Translated by I.A. Ulitkin

$$+\boldsymbol{v}_n(\boldsymbol{k}_{s1}-\boldsymbol{k}_{nm})]t+\varphi_{nm}\}\}, \qquad (1)$$

where A is the amplitude of the incident light field with the wave vector $\boldsymbol{k}$; S_{n1} is the function of radiation scattering by the nth particle in the direction of the wave vector $\boldsymbol{k}_{s1}$; S_{nm1} is the indicatrix of scattering by the nth particle in the direction of the wave vector $\boldsymbol{k}_{s1}$ for light incident on the nth particle from the mth particle; $\boldsymbol{v}_n$ and $\boldsymbol{v}_m$ are the velocities of the nth and mth particles; ω_0 is the central radiation frequency of the laser; Ω is the frequency shift corresponding to the working point on the slope of the transfer function of the frequency–intensity converter, which is a discrimination curve; φ_n is the light wave phase determined by the position of the nth particle in the laser sheet; $\boldsymbol{k}_{nm}$ is the wave vector of the light wave scattered by the mth particle in the direction of the nth particle; $\boldsymbol{v}_m(\boldsymbol{k}_{nm}-\boldsymbol{k})$ is the Doppler frequency shift of the light wave scattered by the mth particle in the direction of the nth particle; $\boldsymbol{v}_n(\boldsymbol{k}_{s1}-\boldsymbol{k}_{nm})$ is the Doppler frequency shift of the light wave with the wave vector $\boldsymbol{k}_{s1}$, scattered by the nth particle and incident from the mth particle side; and φ_{nm} is the light field phase determined by the position of the nth and mth particles in the laser sheet.

The light field (1) scattered by the nth particle and propagating in the direction $\boldsymbol{k}_{s1}$ is transformed by the frequency–intensity converter and detected with a CCD camera. The expression for the intensity of the field producing an image of the nth particle in the frequency-demodulated light scattered in the direction $\boldsymbol{k}_{s1}$ is obtained from (1):

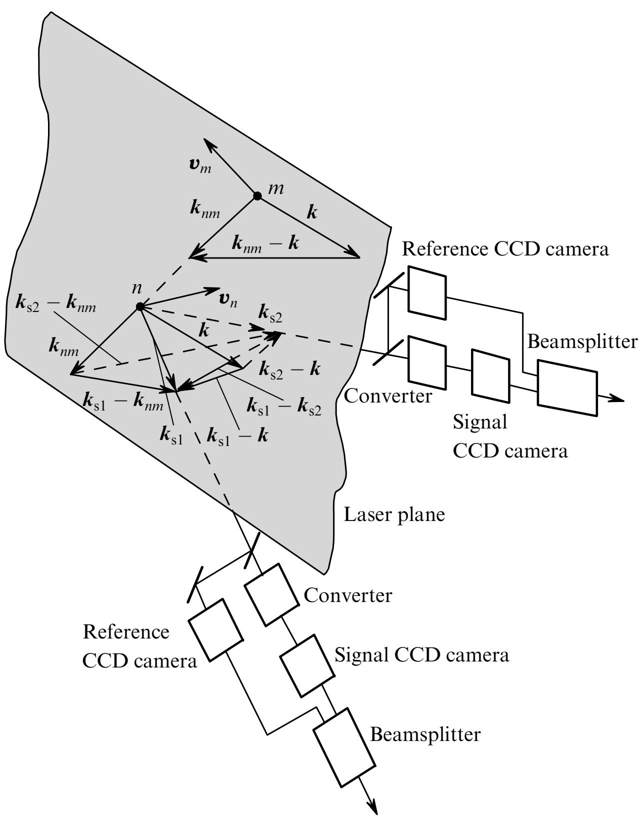

Figure 1. Configuration of light beams in the space of the wave vectors, which illustrates the method of elimination of the influence of multiparticle scattering on the measurement results of the velocity field.

$$i_{n1}=\xi A^2\Big\{S_{n1}^2[\Omega+\boldsymbol{v}_n(\boldsymbol{k}_{s1}-\boldsymbol{k})]$$
$$+\sum_m S_{nm1}^2[\Omega+\boldsymbol{v}_m(\boldsymbol{k}_{nm}-\boldsymbol{k})+\boldsymbol{v}_n(\boldsymbol{k}_{s1}-\boldsymbol{k}_{nm})]\Big\}, \qquad (2)$$

where ξ is the coefficient of the frequency–intensity conversion for the converter. This expression also takes into account that the field intensity at the converter output is proportional to the frequency shift with respect to the working point. In expression (2), the term under the sum sign takes into account the contribution of multiparticle single scattering from adjacent mth particles and determines the error in DGV measurements of the velocity field at the point where the nth particle resides. This partial contribution to the measurement error contains Doppler frequency shifts $\boldsymbol{v}_m(\boldsymbol{k}_{nm}-\boldsymbol{k})$ and $\boldsymbol{v}_n(\boldsymbol{k}_{s1}-\boldsymbol{k}_{nm})$. This contribution is eliminated by introducing the second channel of the particle image detection in the frequency-demodulated light scattered in the direction of the wave vector $\boldsymbol{k}_{s2}$. For the field $\tilde{E}_{n2}$ scattered by the nth particle in the direction of the vector $\boldsymbol{k}_{s2}$, we have the expression

$$\tilde{E}_{n2}=AS_{n2}\exp\{\mathrm{i}\{[\omega_0+\Omega+\boldsymbol{v}_n(\boldsymbol{k}_{s2}-\boldsymbol{k})]t+\varphi_n\}\}$$
$$+A\sum_m S_{nm2}\exp\{\mathrm{i}\{[\omega_0+\Omega+\boldsymbol{v}_m(\boldsymbol{k}_{nm}-\boldsymbol{k})$$
$$+\boldsymbol{v}_n(\boldsymbol{k}_{s2}-\boldsymbol{k}_{nm})]t+\varphi_{nm}\}\}. \qquad (3)$$

Here, S_{n2} and S_{nm2} are the functions of scattering by the nth particle in the direction of the wave vector $\boldsymbol{k}_{s2}$, similar to the functions S_{n1} and S_{nm1}. The light field (3) is transformed by the frequency–intensity converter and detected with a signal CCD camera in the second channel. The expression for the intensity i_{n2} of this field in the frequency-demodulated light scattered in the direction $\boldsymbol{k}_{s2}$ can be derived from (3) by analogy with (2):

$$i_{n2}=\xi A^2\Big\{S_{n2}^2[\Omega+\boldsymbol{v}_n(\boldsymbol{k}_{s2}-\boldsymbol{k})]$$
$$+\sum_m S_{nm2}^2[\Omega+\boldsymbol{v}_m(\boldsymbol{k}_{nm}-\boldsymbol{k})+\boldsymbol{v}_n(\boldsymbol{k}_{s2}-\boldsymbol{k}_{nm})]\Big\}. \qquad (4)$$

Let us substract the image corresponding to expression (4) from the image corresponding to expression (2):

$$i_{n12}=i_{n1}-i_{n2}=\xi A^2\big[\big(S_{n1}^2-S_{n2}^2\big)(\Omega-\boldsymbol{v}_n\boldsymbol{k})$$
$$+S_{n1}^2\boldsymbol{v}_n\boldsymbol{k}_{s1}-S_{n2}^2\boldsymbol{v}_n\boldsymbol{k}_{s2}\big]+\xi A^2$$
$$\times\sum_m\big[\big(S_{nm1}^2-S_{nm2}^2\big)(\Omega+\boldsymbol{v}_{nm}\boldsymbol{k}_{nm}-\boldsymbol{v}_m\boldsymbol{k})$$
$$+S_{nm1}^2\boldsymbol{v}_n\boldsymbol{k}_{s1}-S_{nm2}^2\boldsymbol{v}_n\boldsymbol{k}_{s2}\big]. \qquad (5)$$

Here, $\boldsymbol{v}_{nm}=\boldsymbol{v}_m-\boldsymbol{v}_n$. If the coefficients of scattering by the nth particle in the directions of the wave vectors $\boldsymbol{k}_{s1}$ and $\boldsymbol{k}_{s2}$ are equal, i.e. $S_{n1}^2=S_{n2}^2=S_n^2$ and $S_{nm1}^2=S_{nm2}^2=S_{nm}^2$, we obtain

$$i_{n12}=\xi A^2\Big(S_n^2+\sum_m S_{nm}^2\Big)\boldsymbol{v}_n(\boldsymbol{k}_{s1}-\boldsymbol{k}_{s2}).$$

After normalisation of this expression, we have

$$\tilde{i}_{n12} = \frac{i_{n12}}{\xi A^2\left(S_n^2 + \sum_m S_{nm}^2\right)} = \boldsymbol{v}_n(\boldsymbol{k}_{s1} - \boldsymbol{k}_{s2}). \qquad (6)$$

One can see from (6) that the contribution of the multiparticle scattering is suppressed. The normalised difference of images (6) is determined by the projection of the velocity vector of the nth particle on the difference vector $\boldsymbol{k}_{s1} - \boldsymbol{k}_{s2}$ specifying the direction of the axis of the coordinate-measuring basis.

The conditions $S_{n1}^2 = S_{n2}^2 = S_n^2$ and $S_{nm1}^2 = S_{nm2}^2 = S_{nm}^2$ are fulfilled, for example, in the case of Rayleigh scattering. They are valid for many colloid solutions. For spherical particles, when the directions of the wave vectors $\boldsymbol{k}_{s1}$ and $\boldsymbol{k}_{s2}$ of scattered beams are symmetric with respect to the laser sheet, these conditions are fulfilled because the laser sheet is the symmetry plane for the indicatrix of scattering by the nth particle in the directions $\boldsymbol{k}_{s1}$ and $\boldsymbol{k}_{s2}$. In the particular case of $\boldsymbol{k}_{s2} = -\boldsymbol{k}_{s1} = \boldsymbol{k}_s$, we obtain the configuration of light beams for which expression (6) takes the form

$$\tilde{i}_{n12} = 2\boldsymbol{v}_n\boldsymbol{k}_s. \qquad (7)$$

As follows from (7), in this configuration the normalised image difference of the nth particle in the frequency-demodulated light is unambiguously determined by the projection of the velocity vector of the nth particle on the difference vector $\boldsymbol{k}_{s1} - \boldsymbol{k}_{s2} = 2\boldsymbol{k}_s$ specifying the direction of the coordinate axis in the measuring basis.

The conditions $S_{n1}^2 - S_{n2}^2 = 0$ and $S_{nm1}^2 - S_{nm2}^2 = 0$ are sufficient to eliminate the influence of multiparticle scattering. To fulfil these conditions, it is required to 'seed' the medium under study with spherical particles. In the case of particles of an arbitrary shape, the influence of multiparticle scattering is reduced by averaging frequency-demodulated images (2) and (4) with respect to the particle ensemble during the exposure time. The situation is simplified due to the fact that the method under study does not require producing images of separate particles. The statistical estimates of this effect are presented elsewhere.

Let us estimate the reference signal obtained by using a separate CCD camera. The image of the particle in light scattered in the direction of the wave vector $\boldsymbol{k}_{s1}$ is found from (1):

$$I_{n1} = \left|\tilde{E}_{n1}\right|^2 = A^2\Big|S_{n1}\exp\{\mathrm{i}\{[\omega_0 + \Omega + \boldsymbol{v}_n(\boldsymbol{k}_{s1} - \boldsymbol{k})]t + \varphi_n\}\}$$
$$+ \sum_m S_{nm1}\exp\{\mathrm{i}\{[\omega_0 + \Omega + \boldsymbol{v}_m(\boldsymbol{k}_{nm} - \boldsymbol{k})$$
$$+ \boldsymbol{v}_n(\boldsymbol{k}_{s1} - \boldsymbol{k}_{nm})]t + \varphi_{nm}\}\}\Big|^2 = A^2\Big(S_{n1}^2 + \sum_m S_m^2\Big) + 2A^2 S_{n1}$$
$$\times \sum_m S_{nm1}\cos[\boldsymbol{v}_{nm}(\boldsymbol{k}_{nm} - \boldsymbol{k})t + \varphi_{nm} - \varphi_n] + 2A^2$$
$$\times \sum_{m,q} S_{nm1}S_{nq1}\cos[(\boldsymbol{v}_{nm}\boldsymbol{k}_{nm} + \boldsymbol{v}_{qm}\boldsymbol{k} + \boldsymbol{v}_{nq}\boldsymbol{k}_{nq})t + \varphi_{nm} - \varphi_{nq}],$$

where $\boldsymbol{k}_{nq}$ is the wave vector of a light wave scattered by the qth particle in the direction of the nth particle. In detecting the reference image, averaging during the exposure time and with respect to the ensemble is performed:

$$\langle I_{n1}\rangle = \frac{1}{2}\Big\{\Big\langle A^2\Big(S_{n1}^2 + \sum_n S_{nm1}^2\Big)\Big\rangle + \Big\langle 2A^2 S_{n1}\times$$
$$\times \sum_m S_{nm1}\cos[\boldsymbol{v}_n(\boldsymbol{k}_{nm} - \boldsymbol{k})t + \varphi_n - \varphi_{nm}]\Big\rangle$$
$$+ \Big\langle 2A^2\sum_{m,q} S_{nm1}S_{nq1}\cos[(\boldsymbol{v}_{nm}\boldsymbol{k}_{nm} + \boldsymbol{v}_{qm}\boldsymbol{k} + \boldsymbol{v}_{nq}\boldsymbol{k}_{nq})t$$
$$+ \varphi_{nm} - \varphi_{nq}]\Big\rangle\Big\} = A^2\Big(\langle S_{n1}^2\rangle + \sum_m \langle S_{nm1}^2\rangle\Big). \qquad (8)$$

Thus, for the image of the nth particle in the second channel, we have

$$\langle I_{n2}\rangle = A^2\Big(\langle S_{n2}^2\rangle + \sum_m \langle S_{nm2}^2\rangle\Big). \qquad (9)$$

When the conditions $\langle S_{n1}^2\rangle = \langle S_{n2}^2\rangle = S_n^2$ and $\langle S_{nm1}^2\rangle = \langle S_{nm2}^2\rangle = S_{nm}^2$ are fulfilled according to (8) and (9), we obtain $\langle I_{n1}\rangle = \langle I_{n2}\rangle = A^2(S_n^2 + \sum_m S_{nm}^2)$.

2.2 Formation of a normalised image of the laser sheet in frequency-demodulated scattered light without the use of a reference CCD camera

Consider the formation of a normalised laser-plane image in the frequency-demodulated scattered light with the help of only one CCD camera. Let the frequency – intensity converter have a symmetric transfer function whose examples are shown in Fig. 2. We will select the working points P_1 and P_2 symmetrically located (with respect to the central frequency ω_0) on the linear segments of the transfer function, which perform the role of discrimination curves. Let $\pm\xi$ be the steepness of the frequency discrimination curve in the vicinity of the working points. We will form the laser sheet by two spatially combined and successfully commutated laser beams with frequencies differing by the known quantity 2Ω. The switching frequency $\tilde{\omega}$ of the beams is determined by the Nyquist frequency depending on the width of the spectrum under study. A pair of images of the nth particle is successfully recorded with the CCD camera synchronised with the instant of switching of the beams producing the laser sheet. The expressions for the fields scattered by the nth particle, whose frequencies correspond to the linear parts on the right and left slopes of the transfer function, have the form:

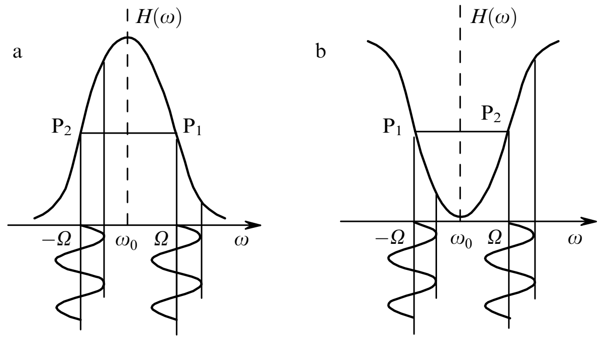

Figure 2. Transfer function $H(\omega)$ of the frequency – intensity converter in the case of its resonance form (a) and in the case of an absorbing cell or multibeam interferometer in reflected light (b).

$$\tilde{E}_n(\boldsymbol{k}_{s1}) = [1 + \mathrm{sgn}(\sin\tilde{\omega}t)]\tilde{E}_{n1}(\Omega, \boldsymbol{k}_{s1}) + [1 - \mathrm{sgn}(\sin\tilde{\omega}t)]E_{n1}(-\Omega, \boldsymbol{k}_{s1}),$$

where

$$\tilde{E}_{n1}(\Omega, \boldsymbol{k}_{s1}) = AS_{n1}\exp\{\mathrm{i}[\omega_0 + \Omega + \boldsymbol{v}_n(\boldsymbol{k}_{s1} - \boldsymbol{k})]t + \mathrm{i}\varphi_n\} + A\sum_m S_{nm1}\exp\{\mathrm{i}[\omega_0 + \Omega + \boldsymbol{v}_m(\boldsymbol{k}_{nm} - \boldsymbol{k}) + \boldsymbol{v}_n(\boldsymbol{k}_{s1} - \boldsymbol{k}_{nm})]t + \mathrm{i}\varphi_{nm}\}; \quad (10)$$

$$\tilde{E}_{n1}(-\Omega, \boldsymbol{k}_{s1}) = AS_{n1}\exp\{\mathrm{i}[\omega_0 - \Omega + \boldsymbol{v}_n(\boldsymbol{k}_{s1} - \boldsymbol{k})]t + \mathrm{i}\varphi_n\} + A\sum_m S_{nm1}\exp\{\mathrm{i}[\omega_0 - \Omega + \boldsymbol{v}_m(\boldsymbol{k}_{nm} - \boldsymbol{k}) + \boldsymbol{v}_n(\boldsymbol{k}_{s1} - \boldsymbol{k}_{nm})]t + \mathrm{i}\varphi_{nm}\}. \quad (11)$$

After the optical frequency demodulation, the camera at the frequency–intensity converter output detects successively in time the images of the nth particle:

$$i_n(\boldsymbol{k}_{s1}) = [1 + \mathrm{sgn}(\sin\tilde{\omega}t)]i_{n1}(\Omega, \boldsymbol{k}_{s1}) + [1 - \mathrm{sgn}(\sin\tilde{\omega}t)]i_{n1}(-\Omega, \boldsymbol{k}_{s1}),$$

where

$$i_{n1}(\Omega, \boldsymbol{k}_{s1}) = \xi A^2 S_{n1}^2[\Omega + \boldsymbol{v}_n(\boldsymbol{k}_{s1} - \boldsymbol{k})] + \xi A^2 \sum_m S_{nm1}^2[\Omega + \boldsymbol{v}_m(\boldsymbol{k}_{nm} - \boldsymbol{k}) + \boldsymbol{v}_n(\boldsymbol{k}_{s1} - \boldsymbol{k}_{nm})]; \quad (12)$$

$$i_{n1}(-\Omega, \boldsymbol{k}_{s1}) = \xi A^2 S_{n1}^2[\Omega - \boldsymbol{v}_n(\boldsymbol{k}_{s1} - \boldsymbol{k})] + \xi A^2 \sum_m S_{nm1}^2[\Omega - \boldsymbol{v}_m(\boldsymbol{k}_{nm} - \boldsymbol{k}) - \boldsymbol{v}_n(\boldsymbol{k}_{s1} - \boldsymbol{k}_{nm})]. \quad (13)$$

These images are stored and subjected to simple linear transformations. By subtracting from the first image the second one, we obtain

$$i_{n12} = i_{n1}(\Omega, \boldsymbol{k}_{s1}) - i_{n1}(-\Omega, \boldsymbol{k}_{s1}) = 2\xi A^2\Big\{\Big(S_{n1}^2 + \sum_m S_{nm1}^2\Big) \times \boldsymbol{v}_n(\boldsymbol{k}_{s1} - \boldsymbol{k}) + \sum_m S_{nm1}^2 \boldsymbol{v}_{nm}(\boldsymbol{k}_{nm} - \boldsymbol{k})\Big\}. \quad (14)$$

Summation of images (12) and (13) yields

$$i_{n1}(\Omega, \boldsymbol{k}_{s1}) + i_{n2}(-\Omega, \boldsymbol{k}_{s1}) = 2\xi A^2\Big(S_{n1}^2 + \sum_m S_{nm1}^2\Big)\Omega. \quad (15)$$

By normalising difference image (14) to total one (15), we find

$$\tilde{i}_{n1}(\boldsymbol{k}_{s1}) = \frac{i_{n1}(\Omega, \boldsymbol{k}_{s1}) - i_{n1}(-\Omega, \boldsymbol{k}_{s1})}{i_{n1}(\Omega, \boldsymbol{k}_{s1}) + i_{n1}(-\Omega, \boldsymbol{k}_{s1})} = \frac{1}{\Omega}\boldsymbol{v}_n(\boldsymbol{k}_{s1} - \boldsymbol{k}) + \frac{\sum_m S_{nm1}^2 \boldsymbol{v}_{nm}(\boldsymbol{k}_{nm} - \boldsymbol{k})}{\Omega\big(S_{n1}^2 + \sum_m S_{nm1}^2\big)}. \quad (16)$$

Expression (16) describes the normalised frequency-demodulated image of the laser sheet produced in a scattered light beam with the wave vector $\boldsymbol{k}_{s1}$. By using an analogous technique, we obtain a normalised frequency-demodulated image of the laser sheet produced in a scattered light beam with the wave vector $\boldsymbol{k}_{s2}$:

$$\tilde{i}_{n2}(\boldsymbol{k}_{s2}) = \frac{i_{n2}(\Omega, \boldsymbol{k}_{s2}) - i_{n2}(-\Omega, \boldsymbol{k}_{s2})}{i_{n2}(\Omega, \boldsymbol{k}_{s1}) + i_{n2}(-\Omega, \boldsymbol{k}_{s1})} = \frac{1}{\Omega}\boldsymbol{v}_n(\boldsymbol{k}_{s2} - \boldsymbol{k}) + \frac{\sum_m S_{nm2}^2 \boldsymbol{v}_{nm}(\boldsymbol{k}_{nm} - \boldsymbol{k})}{\Omega\big(S_{n2}^2 + \sum_m S_{nm2}^2\big)}. \quad (17)$$

When the conditions $S_{n1}^2 = S_{n2}^2 = S_n^2$ and $S_{nm1}^2 = S_{nm2}^2 = S_{nm}^2$ are fulfilled for the difference of the normalised frequency-demodulated nth-particle images corresponding to expressions (16) and (17), we obtain

$$\tilde{i}_{n1}(\boldsymbol{k}_{s1}) - i_{n2}(\boldsymbol{k}_{s2}) = \frac{1}{\Omega}\boldsymbol{v}_n(\boldsymbol{k}_{s1} - \boldsymbol{k}_{s2}). \quad (18)$$

By multiplying (18) by the known quantity Ω, we find

$$\big[\tilde{i}_{n1}(\boldsymbol{k}_{s1}) - \tilde{i}_{n2}(\boldsymbol{k}_{s2})\big]\Omega = \boldsymbol{v}_n(\boldsymbol{k}_{s1} - \boldsymbol{k}_{s2}). \quad (19)$$

One can see from (19) that the influence of multiparticle scattering on the measurement result of the velocity field is eliminated. In this case, the linearity of the measurement scale and broadening of the dynamic range are provided. In the case of particles of an arbitrary shape, the influence of multiparticle scattering is reduced due to the statistical averaging of the difference of normalised converted images (18) produced in different regions of the angular spectrum of scattered light.

The frequency shift 2Ω of commutated beams producing the laser sheet is selected equal to the frequency interval between the working points on the linear segments of the slopes of the symmetrical transfer function. In controlling the transfer function of the frequency – intensity converter, its symmetry condition is not obligatory.

2.3 Control of the transfer function of the frequency – intensity converter

The frequency modulation and the switching of laser beams producing the laser sheet can be used to control the transfer function of the frequency – intensity converter and its locking-in to the laser radiation frequency. Consider the formation of the control signal. We will introduce into the frequency – intensity converter an attenuated part of laser radiation forming the laser sheet. The frequency of this radiation will be converted into the intensity in accordance with the shape of the transfer function. When supplying the switching frequency-modulated light field to the converter input, the light intensity at its output will be described by the expression

$$I = I_0\{1 + \xi\,\mathrm{sgn}(\sin\tilde{\omega}t)[\omega - \omega_0 + \Omega\,\mathrm{sgn}(\sin\tilde{\omega}t)]\}, \quad (20)$$

where I_0 is the intensity of the switching field at the points P_1 and P_2 corresponding to the frequencies $\omega_1 = \omega_0 + \Omega$ and $\omega_2 = \omega_0 - \Omega$; ω is the laser radiation frequency. This intensity is converted, for example, with the help of a photodiode into photoelectric current $J = \rho I$, where ρ is the coefficient taking into account the sensitivity and amplification of the photodiode. It follows from expression (20) that at

$$\omega - \omega_0 + \Omega \, \mathrm{sgn}(\sin \tilde{\omega} t) = 0 \tag{21}$$

the signal $J = \rho I$ is constant ($I = I_0$). This means that the laser radiation frequency and the central frequency of the transfer function of the frequency–intensity converter are matched. If, for some reasons, the laser radiation frequency ω is displaced with respect to the central frequency ω_0 of the converter transfer function by $\Delta\omega$, then (20) taking into account (21) takes the form

$$I = I_0\{1 + \xi \, \mathrm{sgn}(\sin \tilde{\omega} t)[\omega + \Delta\omega - \omega_0 + \Omega \, \mathrm{sgn}(\sin \tilde{\omega} t)]\}$$

$$= I_0\{1 + \Delta\omega \xi \, \mathrm{sgn}(\sin \tilde{\omega} t)\}. \tag{22}$$

As follows from (22), when the frequencies of the converter output are misbalanced, there appears a variable signal whose frequency is equal to the switching frequency of the light field and whose amplitude is proportional to the frequency detuning $\Delta\omega$ and the sign corresponds to that of the frequency detuning. This signal at the frequency $\tilde{\omega}$ can be used as an error signal in forming the control signal in the system of automatic frequency adjustment. The steepness of the discrimination characteristics ξ is determined by the amplitude of the control signal $\tilde{I}(\Delta\omega)$ at a given frequency detuning $\Delta\omega$: $\xi = \tilde{I}(\Delta\omega)/\Delta\omega$. Scanning $\Delta\omega$ we can obtain the profile of the converter transfer function.

Figure 3 shows an example of a simplified scheme of an optical Doppler visualizer of the velocity field with the elimination of the influence of multiparticle scattering on the measurement result. The laser sheet is formed by an anamorphic optical system comprising lenses 1, 2, and 3. Frequency modulation and switching of laser beams producing the laser sheet are performed with the help of an acousto-optic travelling-wave modulator operating in the Bragg regime. This modulator is controlled by an electric signal $U \, \mathrm{sgn}(\sin \tilde{\omega} t) \cos 2\Omega t$ from the a computer-controlled generator. The commutated Bragg diffraction orders are spatially combined with lens 2 and a Wollaston prism. The angle between the diffracted commutated beams is equal to the splitting angle of the Wollaston prism, which combines optical beams in space. Half-wave phase plate 1 matches polarisations of the diffracted beams with the Wollaston prism orientation. Quarter-wave phase plate 2 produces the circularly polarised laser beams. Converters 1, 2 and CCD cameras 1, 2 are mounted, respectively, in the direction of the wave vectors $\boldsymbol{k}_{s1}$ and $\boldsymbol{k}_{s2}$, whose difference $\boldsymbol{k}_{s1} - \boldsymbol{k}_{s2}$ specifies the axis direction of the coordinate-measuring basis. The frequency–intensity conversion is performed in each channel in the single-chamber regime. The PC converts the frequency-demodulated images. The central frequency of the transfer function is automatically adjusted for each converter to the laser radiation frequency. The frequency-modulated light signal used to control the transfer function can be coupled into the converter with the help, for example, of a fibre or a fixed scattering reference placed in the laser sheet. The spatial configuration of scattered beam and the laser sheet in Fig. 3 are exemplary and can be changed under conditions of a real experiment.

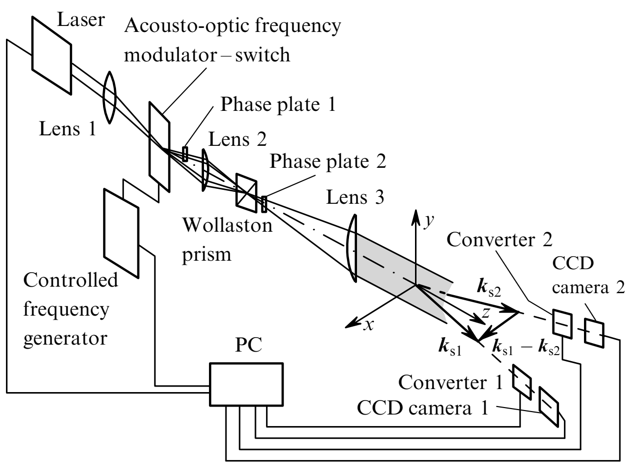

Figure 3. Example of the optical scheme of the DGV system suppressing the influence of multiparticle scattering on the measurement of the velocity field.

3. Conclusions

We have described the method of laser Doppler visualisation and measurement of the velocity field in gas and liquid flows with the suppression of the influence of multiparticle scattering. Minimisation of the influence of multiparticle scattering is based on obtaining differential combinations of normalised frequency-demodulated images of the laser sheet in different regions of the angular spectrum of scattered light. We have shown the possibility of using one CCD camera for producing a normalised image of the laser sheet in the frequency-demodulated scattered light. In this case, the laser sheet is formed by two spatially combined and successively commutated laser beams whose frequencies differ by the known quantity matched with the width of the transfer function of the frequency–intensity converter at a given level. The switching frequency of the laser beams is the error signal frequency in forming the control signal in the system of automatic adjustment of the central frequency of the transfer function to the laser radiation frequency and control of its profile.

Acknowledgements. This work was supported by the German Centre of Aviation and Astronautics.

References

1. Drain L.E. *The Laser Doppler Technique* (New York: Wiley, 1980).
2. Dubnishchev Yu.N., Rinkevichus B.S. *Metody lazernoi doplerovskoi anemometri* (Methods of Laser Doppler Anemometry) (Moscow: Nauka, 1982).
3. Dubnishchev Yu.N. *Lazernye doplerovskie izmeritel'nye tekhnologii* (Laser Doppler Measurement Techniques) (Novosibirsk: izd-vo NGTU, 2002).
4. Belousov P.Ya., Dubnishchev Yu.N. Soviet Patent No. 567141. *Bulletin of Inventions*, No. 28 (1977).
5. Belousov P.Ya., Dubnishchev Yu.N., Pal'chikov I.G. *Opt. Spektrosk.*, **52**, 876 (1982).
6. Belousov P.Ya., Dubnishchev Yu.N. *Opt. Laser Technol.*, **9**, 229 (1977).
7. Belousov P.P., Belousov P.Ya., Dubnishchev Yu.N. *Kvantovaya Elektron.* **29**, 157 (1999) [*Quantum Electron.*, **29**, 995 (1999)].
8. Belousov P.P., Belousov P.Ya., Dubnishchev Yu.N. *Pis'ma Zh. Tekh. Fiz.*, **28** (16), 6 (2002).
9. Dubnishchev Yu.N., Belousov P.P., Belousov P.Ya. *Techn. Phys. Lett.*, **30**, 313 (2004).
10. Komine H. USA Patent No. 4919536 (1990).
11. Fisher A., Buttner L., Czarske J., Eggert M., Grosche G., Miller H. *Meas. Sci. Tecnol.*, **18**, 2529 (2007).